NASA/TM—2010-215669

Development and Life Prediction of Erosion Resistant Turbine Low Conductivity Thermal Barrier Coatings

Dongming Zhu, Robert A. Miller, and Maria A. Kuczmarski
Glenn Research Center, Cleveland, Ohio

February 2010

NASA STI Program . . . in Profile

Since its founding, NASA has been dedicated to the advancement of aeronautics and space science. The NASA Scientific and Technical Information (STI) program plays a key part in helping NASA maintain this important role.

The NASA STI Program operates under the auspices of the Agency Chief Information Officer. It collects, organizes, provides for archiving, and disseminates NASA's STI. The NASA STI program provides access to the NASA Aeronautics and Space Database and its public interface, the NASA Technical Reports Server, thus providing one of the largest collections of aeronautical and space science STI in the world. Results are published in both non-NASA channels and by NASA in the NASA STI Report Series, which includes the following report types:

- TECHNICAL PUBLICATION. Reports of completed research or a major significant phase of research that present the results of NASA programs and include extensive data or theoretical analysis. Includes compilations of significant scientific and technical data and information deemed to be of continuing reference value. NASA counterpart of peer-reviewed formal professional papers but has less stringent limitations on manuscript length and extent of graphic presentations.

- TECHNICAL MEMORANDUM. Scientific and technical findings that are preliminary or of specialized interest, e.g., quick release reports, working papers, and bibliographies that contain minimal annotation. Does not contain extensive analysis.

- CONTRACTOR REPORT. Scientific and technical findings by NASA-sponsored contractors and grantees.

- CONFERENCE PUBLICATION. Collected papers from scientific and technical conferences, symposia, seminars, or other meetings sponsored or cosponsored by NASA.

- SPECIAL PUBLICATION. Scientific, technical, or historical information from NASA programs, projects, and missions, often concerned with subjects having substantial public interest.

- TECHNICAL TRANSLATION. English-language translations of foreign scientific and technical material pertinent to NASA's mission.

Specialized services also include creating custom thesauri, building customized databases, organizing and publishing research results.

For more information about the NASA STI program, see the following:

- Access the NASA STI program home page at *http://www.sti.nasa.gov*

- E-mail your question via the Internet to *help@sti.nasa.gov*

- Fax your question to the NASA STI Help Desk at 443–757–5803

- Telephone the NASA STI Help Desk at 443–757–5802

- Write to:
  NASA Center for AeroSpace Information (CASI)
  7115 Standard Drive
  Hanover, MD 21076–1320

NASA/TM—2010-215669

Development and Life Prediction of Erosion Resistant Turbine Low Conductivity Thermal Barrier Coatings

Dongming Zhu, Robert A. Miller, and Maria A. Kuczmarski
Glenn Research Center, Cleveland, Ohio

Prepared for the
65th Annual Forum and Technology Display
sponsored by the American Helicopter Society
Grapevine, Texas, May 27–29, 2009

National Aeronautics and
Space Administration

Glenn Research Center
Cleveland, Ohio 44135

February 2010

Acknowledgments

The work was supported by NASA Fundamental Aeronautics Program (FAP) Subsonic Rotary Wing (SRW) project. The authors are grateful to Mr. Michael Perez for performing the burner rig erosion tests.

This work was sponsored by the Fundamental Aeronautics Program
at the NASA Glenn Research Center.

Level of Review: This material has been technically reviewed by technical management.

Available from

NASA Center for Aerospace Information
7115 Standard Drive
Hanover, MD 21076–1320

National Technical Information Service
5301 Shawnee Road
Alexandria, VA 22312

Available electronically at http://gltrs.grc.nasa.gov

Development and Life Prediction of Erosion Resistant Turbine Low Conductivity Thermal Barrier Coatings

Dongming Zhu, Robert A. Miller, and Maria A. Kuczmarski
National Aeronautics and Space Administration
Glenn Research Center
Cleveland, Ohio 44135

Abstract

Future rotorcraft propulsion systems are required to operate under highly-loaded conditions and in harsh sand erosion environments, thereby imposing significant material design and durability issues. The incorporation of advanced thermal barrier coatings (TBC) in high pressure turbine systems enables engine designs with higher inlet temperatures, thus improving the engine efficiency, power density and reliability. The impact and erosion resistance of turbine thermal barrier coating systems are crucial to the turbine coating technology application, because a robust turbine blade TBC system is a prerequisite for fully utilizing the potential coating technology benefit in the rotorcraft propulsion. This paper describes the turbine blade TBC development in addressing the coating impact and erosion resistance. Advanced thermal barrier coating systems with improved performance have also been validated in laboratory simulated engine erosion and/or thermal gradient environments. A preliminary life prediction modeling approach to emphasize the turbine blade coating erosion is also presented.

Introduction

Advanced thermal barrier coatings (TBC) are critical for designing next generation rotorcraft turbine engines because of their ability to allow increased engine gas temperatures and reduced cooling requirements, thus helping to achieve improved engine performance and durability. Multicomponent, oxide-defect-cluster based low conductivity thermal barrier coatings, combined with improved single crystal Ni-base superalloys, have demonstrated feasibility for increasing gas turbine engine blade temperature capability and reducing cooling requirements (Refs. 1 to 4). A recent systems assessment has shown that advanced turbine thermal barrier coatings can provide significant benefits in increasing engine efficiency (Ref. 5). However, a prime-reliant coating design approach is necessary to take full advantage of the thermal barrier coating technology in future rotorcraft engine systems. In particular, turbine blade thermal barrier coatings are especially susceptible to engine ingested sand erosion and impact damages because of the high velocity flow path nature of the blades and complex particulate-coating interactions under high heat-flux combustion turbine environments. Although significant advances have been made in thermal barrier coating technologies for reduced thermal conductivity, increased temperature capability and improved cyclic durability, erosion and impact resistance improvements of the coating systems have remained one of the most significant challenges for the turbine thermal barrier coating developments and applications. Advanced turbine blade thermal barrier coatings are currently being developed under the NASA Rotary Wing Project aimed at increasing the coating toughness and erosion resistance, in order to meet future engine design and performance requirements. Extensive research efforts have been made in developing new coating compositions, coating processing, and erosion mechanism models in order to improve the turbine coating erosion and impact durability (Refs. 6 and 7). The main objective of this effort is to develop higher toughness turbine TBC systems with increased erosion and impact resistance for rotorcraft propulsion engines. The performance of advanced turbine blade thermal barrier coating systems, designed based on nano-tetragonal phase toughening approaches, will be discussed. These are based on the newly established erosion burner rig testing in simulated sand ingestion environments. Emphasis will also be placed on the more engine relevant long-term, high-temperature smaller particulate erosion conditions, so the erosion mechanisms can be investigated for developing the turbine blade coating life models.

Experimental Procedures

Advanced Thermal Barrier Coatings

Advanced ceramic thermal barrier coatings were designed using a multicomponent defect-clustering approach to achieve the required low conductivity, high-temperature stability and improved durability (Refs. 1 to 3). In this study, the high temperature erosion and impact performance of oxide-clustering thermal barrier coating systems including ZrO_2-Y_2O_3-Gd_2O_3-Yb_2O_3 (t' ZrYGdYb) and ZrO_2-Y_2O_3-Gd_2O_3-Yb_2O_3-TiO_2-Ta_2O_5 (t' ZrYGdYbTT) was investigated. The advanced TBC systems, typically consisting of a 130 to 200 μm thick ceramic top coat and a 75 to 100 μm thick PtAl intermediate bond coat, were electron beam-physical vapor deposited (EB-PVD) on to 25.4 mm diameter disk Rene N5 nickel-base superalloy substrates. The coating compositions were chosen based on nano-tetragonal phase toughening design criteria and previous, preliminary phase stability/durability test results, aiming to improve the erosion resistance of the low conductivity thermal barrier coatings. The advanced t' coatings were also compared with the

baseline ZrO_2-7wt%Y_2O_3 (7YSZ), and cubic phased coatings ZrO_2-4mol%Y_2O_3-3mol%Gd_2O_3-3mol%Yb_2O_3 (cubic 433 ZrYGdYb), ZrO_2-4mol%Y_2O_3-3mol%Gd_2O_3-3mol%Yb_2O_3-TiO_2-Ta_2O_5 (cubic 433 ZrYGdYbTT), ZrO_2-4mol%Y_2O_3-4mol%Gd_2O_3-4mol%Yb_2O_3 (cubic 444 ZrYGdYb), and pyrochlore ($Zr_2Gd_2O_7$) coatings. The EB-PVD coatings were all deposited using pre-fabricated evaporation ingots made using the designed compositions.

Erosion Burner Rig and Testing

A Mach 0.3 to 1.0 high velocity burner rig with erosion capability was developed for advanced turbine blade thermal barrier coating testing in a laboratory simulated turbine engine relevant erosion environments. Early work has demonstrated the burner rig effectiveness in evaluating the erosion behavior of ceramic seal coats and thermal barrier coatings (Refs. 8 and 9). The rig development in this work has emphasized increasing the erodent particle velocities at high temperatures by increased gas mass flow rate, erodent flow uniformity with improved feeding systems and a duct approach, and more relevant thermal gradient turbine environments.

As can be seen in Figure 1, the high velocity burner erosion rig consists of a Jet fuel combustor, a 19 mm (3/4 in.) diameter highly efficient burner nozzle, a specimen holder fixture and precision erodent feeder, and jet fuel and preheated compressed air supplies. The burner nozzle inner surface contour was designed based on an ANSI/ASME nozzle standard to achieve better flame stability and uniformity (Ref. 10), with the overall configuration modified for accommodating increased burner mass flow and higher heat flux environments. The nozzle was made of a single crystal nickel-base superalloy turbine blade material to ensure high temperature durability.

To achieve high erosion particle velocities, a computational fluid dynamics modeling (CFD) approach in conjunction with experimental investigations was employed to optimize the burner and erodent injection design. The CFD model (Fluent) was used to calculate the gas and particle velocities for the burner rig temperatures and pressures of interest. The modeling and experimental testing were conducted in relative burner velocities ranging from Mach 0.3 to 0.9, representative to turbine engine conditions. Al_2O_3 particles were used as erodent and the particle sizes used were ranged from 27 to 560 μm in order to understand the coating broad erosion and impact behavior. A modified burner rig configuration with an extension duct (300 mm in length and 19 mm inner diameter) was also explored to further accelerate the erodent particle and increase the velocity.

The coating erosion evaluations was mostly conducted at 1800 °F (coating surface ~1900 °F) and 2000 °F (coating surface 2100 °F), respectively, using 27 μm size Al_2O_3 particles, but also compared with tests performed at 2200 °F using 50 and 560 μm size Al_2O_3 particles. The erosion rate was determined by interrupted coating erosion thickness-recession and weight-loss measurements, and also by the erodent amount required for the coating erosion penetration.

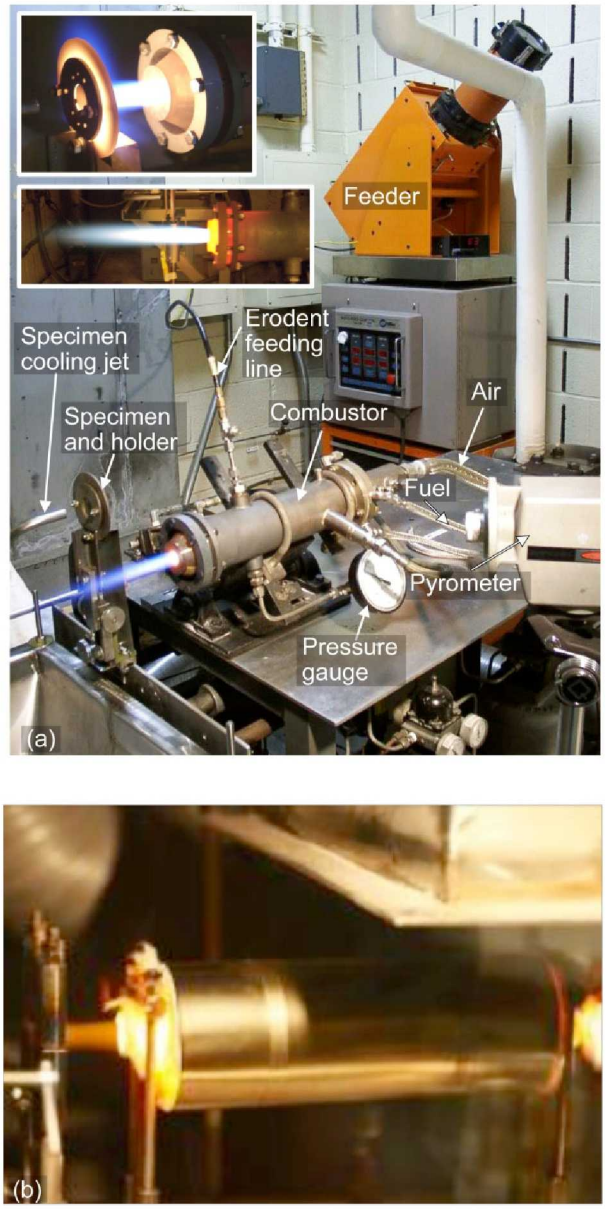

Figure 1.—Mach 0.3-1.0 high velocity burner erosion rig. (a) The burner rig for the coating erosion testing. The insets show the burner nozzle under test operation of Mach 0.9. (b) The burner rig coating erosion testing for coating erosion model validation. The burner and duct system can significantly improve the flow uniformity and erodent velocities for the erosion testing.

Experimental Results and Discussion

Burner Rig Modeling and Characterization

Figure 2(a) shows the particle velocities modeled for a 27 μm erodent size using the CFD analysis in Mach 0.3 and 0.5 burner conditions, respectively. It can be seen that the particle velocity increases with the distance from the burner nozzle exit and burner gas velocity (Mach number). At 25 mm (1 in.) distance, the particle velocity was estimated at 105 and 200 m/s, respectively, under the Mach 0.3 and Mach 0.5 burner gas flows. The maximum velocity is reached at 0.1 m distance from the burner nozzle exit. The modeling is in a good agreement with the experimental measurements, as show in Figure 2(b) and (c).

For larger erodent particle size cases, lower particle velocities are expected at a given burner Mach number and longer acceleration distance is needed. As can be seen from Figure 3 CFD modeling results, the velocities are approximately 20 and 100 m/s at 25 mm distance from the nozzle injector for the 50 and 560 μm particle sizes, respectively under burner Mach 0.4 condition. The maximum velocities can be reached in roughly 0.2 m from the nozzle exit for the large particle size.

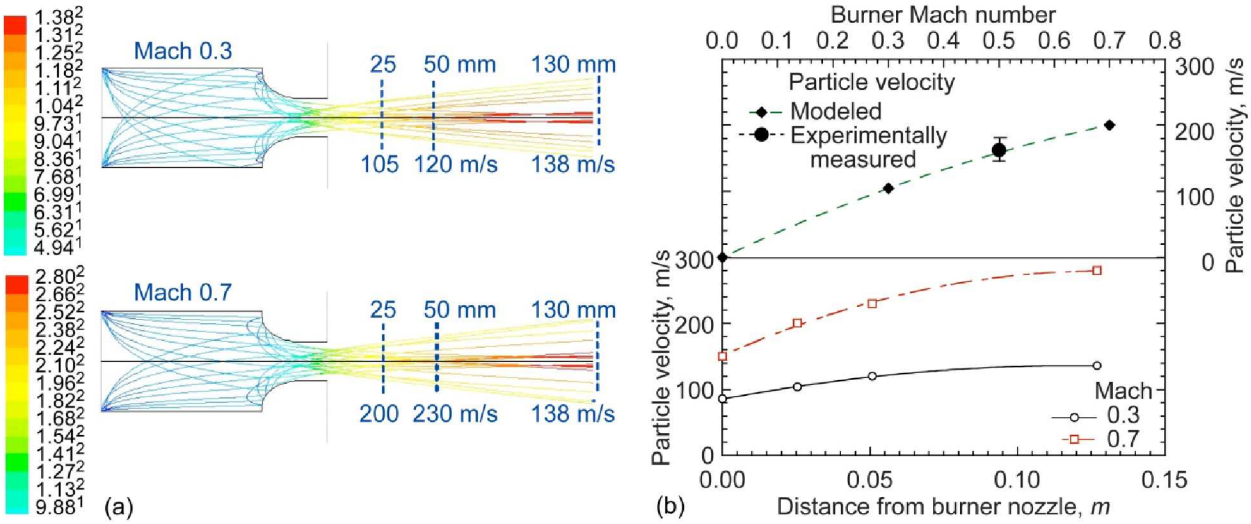

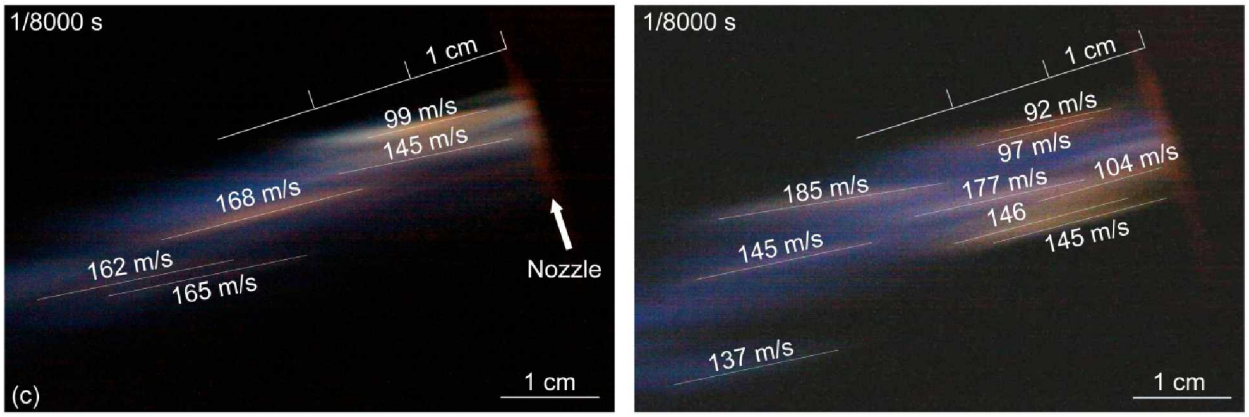

Figure 2.—(a) The CFD modeled particle velocities for 27 μm size particles under Mach 0.3 and Mach 0.7 burner operating conditions. (b) Modeled particle velocity as compared with experimental measurements. (c) Representative photographs of the particle velocity measurements at Mach 0.5. The images were intentionally tilted to cover a larger field of view while maintaining high resolution to resolve small high velocity erodent particles.

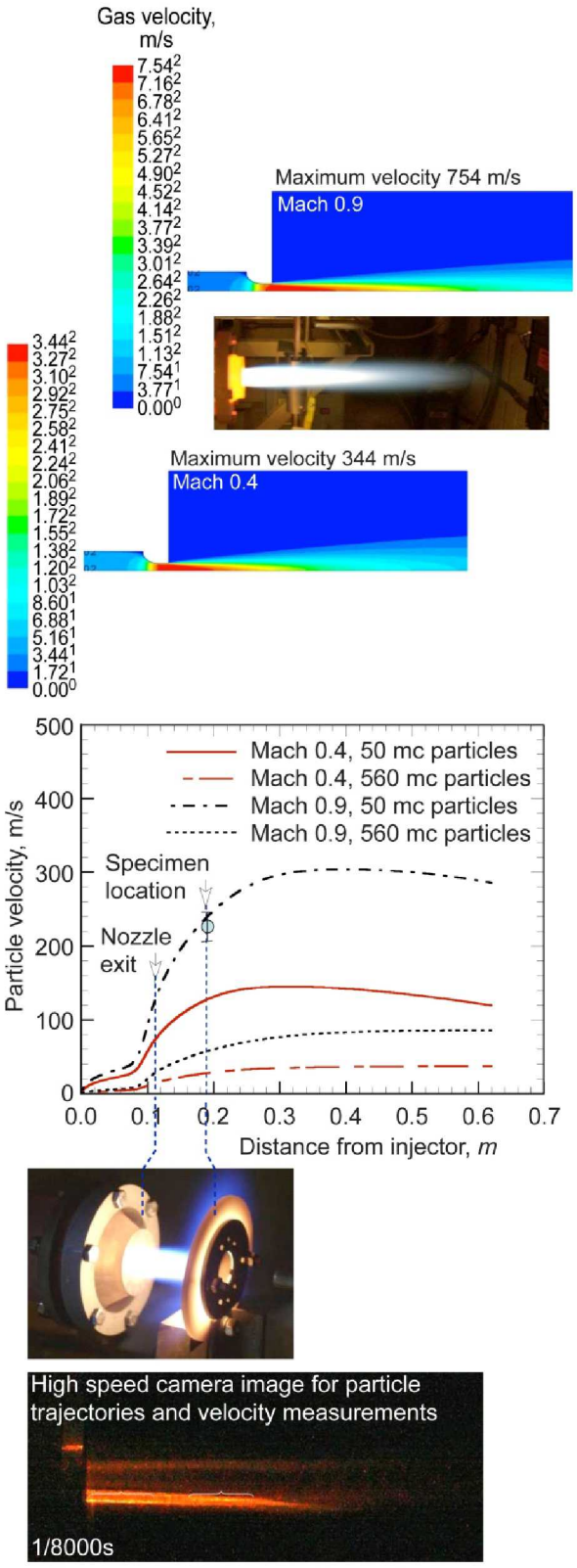

Figure 3.—Particle velocities modeling based on CFD analysis for 50 and 560 μm size particles under burner Mach 0.4 and 0.9 conditions, and validated by experiments.

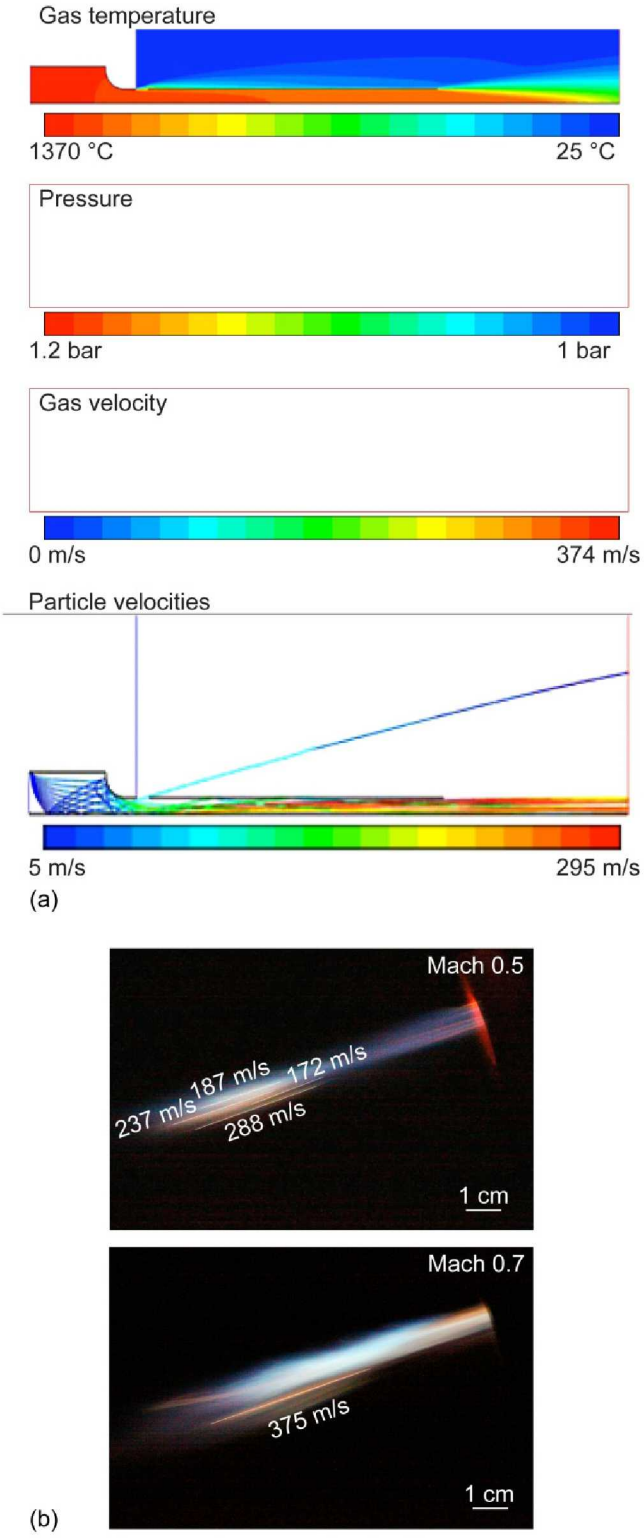

Figure 4.—Ducted rig particle velocity analysis and measurements for 27 μm size particles. (a) CFD modeling. (b) Burner particle velocity measurements.

Thermal Barrier Coating Erosion Behavior

Figure 5 shows the typical erosion rate behavior of the thermal barrier coatings at high temperatures. It can be seen that the coatings usually have a higher initial erosion rate, followed by a slower steady-state erosion rates. The decreased steady-state erosion is due to some coating sintering and densification of the very surface coating layers that have higher erosion resistance. The coating erosion rates become faster at the third stage when the coatings are at near the failure stage.

The coating erosion behavior of various turbine thermal barrier coatings are summarized in Figure 6, as expressed as erosion rate (defined here as 25 μm coating thickness recession per gram erodent required). It can be seen that erosion rates of the coatings typically had some variability, largely influenced by coating composition and processing variations, and especially for the new multicomponent coating systems. The baseline 7YSZ coatings had more consistent erosion behavior.

In order to further increase the particle velocities and uniformity, the burner rig was also modified with an additional duct as shown in Figure 1(b). The CFD model predicts that the particle velocities can be increased from 150 m/s to over 250 m/s for the 27 μm particles under Mach 0.5 conditions. The particle velocities were also confirmed by experiments measurement, as shown in Figure 4(b).

As compared to the baseline 7YSZ coating, the cubic phased coating systems (cubic 433-ZrYGdYb, cubic 433-ZrYGdYb 5-5TiTa, and pyrochlore based coatings) showed the fastest erosion rates. Due to higher yield strength and therefore lower toughness, it would be expected that the cubic phase coatings had the lowest erosion rates. The lower phase stability coating with t' + monoclinic phase ZrRETT due to the lower Gd, Yb dopant additions in the presence of Ti and Ta also showed higher erosion rates. The well processed low conductivity turbine t' coating systems (both t' ZrYGdYb and ZyYGdYbTT) with reasonably controlled composition homogeneity) generally showed improved erosion resistance (lower erosion rates) as compared to the baseline 7YSZ in both 27 and 50 μm size erosion and 560 μm impact tests. Advanced processed low k coatings have shown significantly improved erosion resistance.

The test results showed that the coating erosion rate generally increases with erodent particle size tested in the Mach 0.5 to 0.7 range. For the 27 μm size particles, the coating erosion rates *decreased* dramatically in higher temperature tests (coating temperature 2100 °F) compared to the lower temperature (coating temperature 1900 °F). The significantly increased plasticity of the t' based coatings at the higher temperature can contribute to the increased erosion resistance.

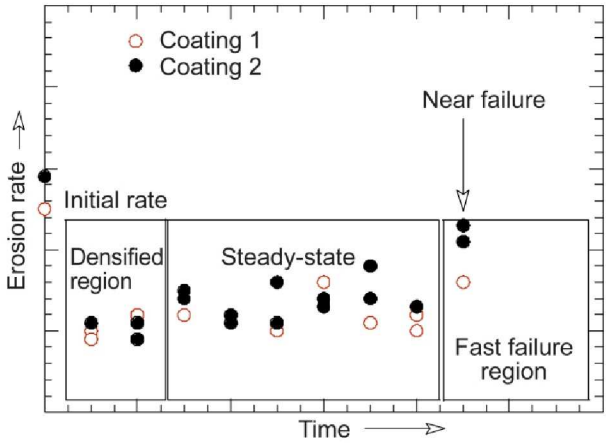

Figure 5.—Typical erosion rate regimes of thermal barrier coatings. The coating erosion can be characterized by an initial fast erosion stage, a slower "steady-state" erosion stage, and a third faster erosion stage near failure.

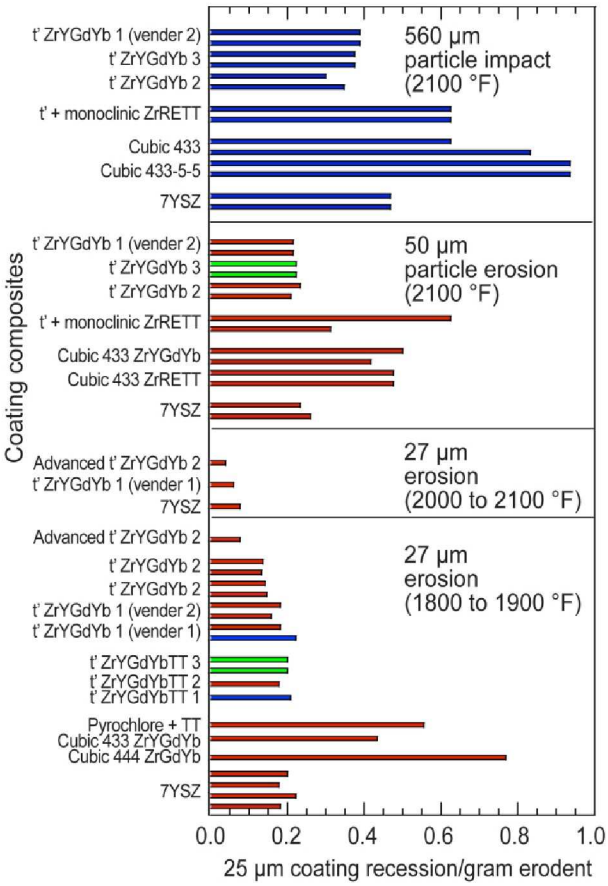

Figure 6.—The erosion behavior of turbine thermal barrier coatings of various low conductivity coatings as compared to baseline coating 7YSZ under various test conditions.

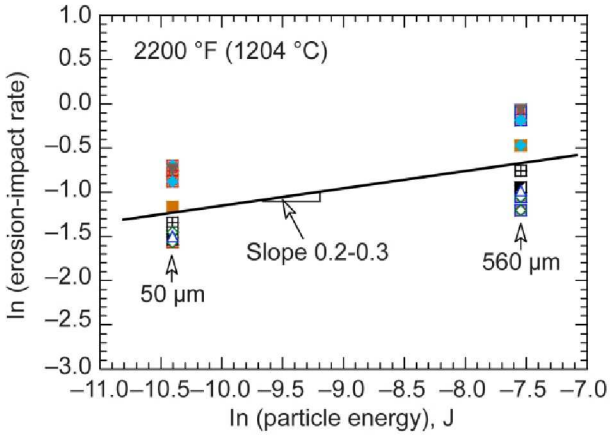

Figure 7.—The relative erosion-impact rate dependence for 50 and 560 µm sized erodent particles for selected coating systems tested at 2200 °F (1204 °C).

Figure 7 shows the particle energy dependence of the erosion/impact rates, for 50 and 560 µm size erodent particles tested at 2200 °F (1204 °C). The ln (erosion-impact rates) - ln (particle energy) plot allows the determination of the energy exponent of the erosion/impact rates. It can be seen that the high temperature data showed relatively low energy dependence. The average slope of the fitted lines for the selected coating systems is found to be approximately 0.21±0.04. It should be noted that the two particle size cases represent two distinct coating damage and failure mechanism regimes (with the 50 µm size particles as the erosion dominant mechanism and 560 µm size particles as the impact damage mechanism). Nevertheless, it does provide some information on the complexity of the coating general erosion behavior. Figure 8 shows the erosion and impact surface morphologies of low conductivity tetragonal phase t' ZrYGdYb coatings. It can be seen from Figure 8(a) that, in the 50 µm particle erosion case, the ceramic coating is characterized by minor surface plastic deformation and densification resulting from the particle impingement. The coating erosion is primarily caused by small-area and shallow-depth spalling under the repetitive erodent particle loading. However, in the 560 µm particle impact case as shown in Figure 8(b), the coating surface typically experiences significant plastic deformation and densification. It can be concluded that the high temperature plastic deformation or plasticity can lead to increased coating toughness and the energy absorption for the 560 µm size particles impact case, therefore leading to the low energy exponent for the coating systems observed in this study. Severe surface plasticity observed for the 560 µm size coating impact testing case supports the hypothesis of the increased coating toughness and reduced erosion/impact rates for the large particles at the high temperatures. It should be noted that large-area and deep-coating layer spallation can occur especially at the late stage of the impact process due to the increased coating delamination driving force and accumulated damage under high impact energy conditions.

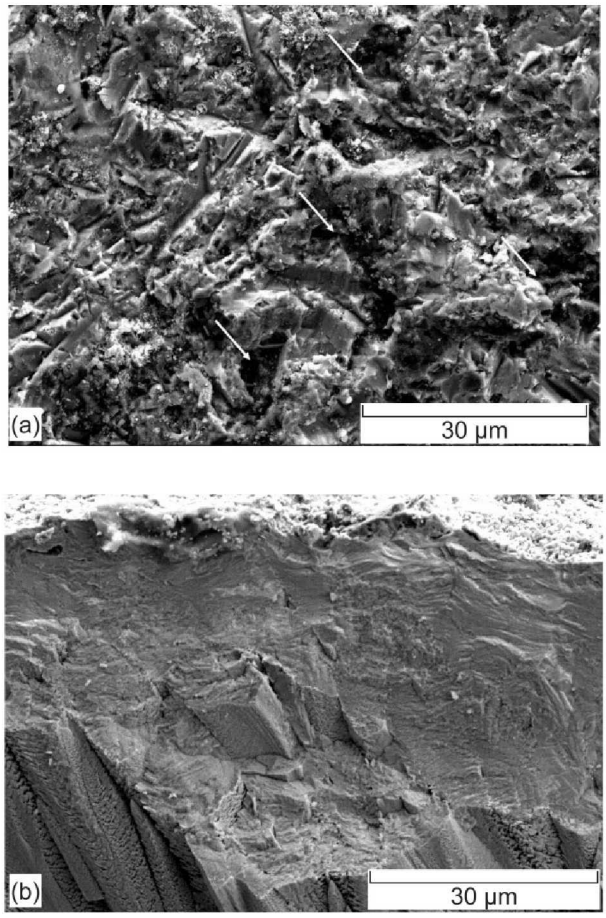

Figure 8.—Scanning electron microscope images showing surface damage morphologies of high toughness low conductivity thermal barrier coatings under erosion and impact testing, respectively. (a) Erosion surface with limited surface plasticity and small area erosion-fatigue spalling (arrows showing the coating spallation areas). (b) Impact surface with extensive surface plasticity and large area spalling.

Thermal Barrier Coating Erosion Life Prediction

The erosion modeling is focused on the effect of the underlying thermal barrier coating properties on the high temperature erosion behavior. It has been shown that the TBC erosion modeling and life models can be achieved by strain amplitudes of various degradation mechanisms in conjunction with fracture mechanics approaches.

The strain amplitude model is given by

$$\Sigma\left(\Delta\varepsilon_{p,\text{eroson}}, \Delta\varepsilon_{p,\text{creep}}, \Delta\varepsilon_{p,\text{heat\_flux}}, \Delta\varepsilon_{p,\text{LCF}}, \Delta\varepsilon_{p,\text{oxidation}}\right) \cdot N_f^{1/2} = \varepsilon_c \quad (1)$$

Where $\Delta\varepsilon_{p,\text{erosion}}$ is the average repetitive particulate erosion induced strain amplitude per particulate impact, $\Delta\varepsilon_{p,\text{creep}}$, $\Delta\varepsilon_{p,\text{heat\_flux}}$, $\Delta\varepsilon_{p,\text{LCF}}$, and $\Delta\varepsilon_{p,\text{oxidation}}$ are coating sintering-creep,

heat flux strain gradient and applied low cycle fatigue and oxidation *plastic* strain induced strain amplitudes, respectively. The thermal barrier coating erosion rate $\Delta\varepsilon_{p,\text{erosion}}$ $\dot{\varepsilon}_{p,erosion}$, defined as the mass loss from the coating per unit mass erodent, can be determined from the erodent particle kinetic energy and coating deformation volume based on Equation (1)

$$\dot{\varepsilon}_{p,\text{erosion}} = m_{\text{erodent}} \cdot C \cdot f(\alpha) \cdot V_{\text{erodent}}^{n} \tag{2a}$$

$$\dot{\varepsilon}_{p,\text{erosion}} = K \cdot \frac{\rho_{\text{TBC}} \cdot \rho_{\text{erodent}}^{1/2} \cdot V^{n}}{\varepsilon_c^2 \cdot H(T)^{3/2}} \tag{2b}$$

Where m_{erodent} is the erodent mass, $f(\alpha)$ is the impingement angle function, C, K are constants, n is the erodent velocity exponent, typically n = 2–3 depending on the extent of deformation occurred, ρ_{TBC} and ρ_{erodent} are the densities of the thermal barrier coating and erodent, respectively, and V is erodent velocity, $H(T)$ is the temperature dependent dynamic hardness of the coating. Given the coating defect size can be typically assumed on the magnitude of the column width w, the Equation (2b) can be rewritten in terms of the coating toughness

$$\dot{\varepsilon}_{p,\text{erosion}} = K_1 \cdot \frac{\rho_{\text{TBC}} \cdot w \cdot E_{\text{TBC}} \cdot \rho_{\text{erodent}}^{1/2} \cdot V^{n}}{G_c \cdot H(T)^{3/2}} \tag{3}$$

Where G_c is the critical strain energy release rate of the coating. It can be seen that the erosion rate can be reduced by increasing the coating toughness G_c, which can be achieved by the coating compositional design and processing improvements. Since the sintered coating hardness decreases significantly with temperature based on our previous experimental and modeling work, as shown in Figure 9, the erosion rate temperature dependence will be governed by two competing factors, that is, the erosion rate increases with the overall coating softening (which increases the coating erosion rate) and decreases with increased coating toughness due to the increased plastic deformation (which reduces the coating erosion rate). As mentioned above, the significantly reduced erosion rates were observed at higher testing temperature (2100 °F) as compared to those at lower testing temperature (1900 °F). The reduction in erosion rates was attributed to the predominant plasticity occurring at the higher temperature and therefore increased coating toughness. The preliminary coating development work demonstrated that the coating toughness improvements through new compositional and microstructural design and processing optimization that can increase the erosion resistant up to 80 to 100 percent at high temperatures. The coating erosion rate and life prediction will focus on characterizing the effective coating toughness and microstructural level coating properties to establish physics-based models.

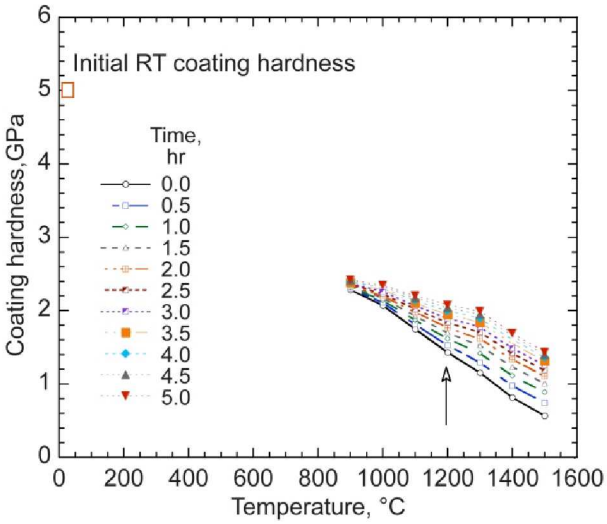

Figure 9.—Turbine TBC hardness values as a function of time at various temperatures, modeled from the high temperature strength measurements and sintering kinetics of the coating systems. The higher temperature resulted in more rapid hardness increases due to sintering, although the overall hardness values are lower compared to those at lower temperatures, due to the ZrO_2 softening behavior.

Concluding Remarks

An advanced high velocity burner rig based erosion test approach has been established to evaluate the turbine thermal barrier coatings in relevant engine environments. CFD models have been established to understand gas and erodent flows for the burner rig conditions.

A new series of t' phase rare earth oxide (Gd_2O_3 and Yb_2O_3 codoped)- and TiO_2/Ta_2O_5-alloyed, ZrO_2-based thermal barrier coatings were designed and processed. The advanced turbine thermal barrier coatings developed for rotorcraft engines will have combined low conductivity and high toughness for improved thermal barrier performance and erosion resistance. The coating systems demonstrated initial improvements in the erosion resistance. The long-term durability of the turbine airfoil thermal barrier coating systems will be evaluated to develop comprehensive physics-based life prediction models addressing the erosion, sintering and fatigue interactions and strain damage accumulations, and to validate the models for turbine blade components.

References

1. Dongming Zhu, and Robert A. Miller, "Low Conductivity and Sintering Resistant Thermal Barrier Coatings," US Patent No. 6,812,176, 2004; US Patent No. 7,001,859, 2006; US Patent No. 7,186,466, 2007.
2. Dongming Zhu, and Robert A. Miller, "Thermal Conductivity and Sintering Behavior of Advanced

Thermal Barrier Coatings," Ceram. Eng. Sci. Proc., vol. 23 (2002), pp. 457–468.
3. Dongming Zhu and Robert A. Miller, "Development of Advanced Low Conductivity Thermal Barrier Coatings," International Journal of Applied Ceramic Technology, vol. 1 (2004), pp. 86–94.
4. Dongming Zhu et al., "Thermal and Environmental Barrier Coating Development for Advanced Propulsion Engine Systems," AIAA–2007–2130, 48th AIAA/ASME/ASCE/AHS/ASC Structures, Structural Dynamics, and Materials Conference, 23–26 April 2007, Honolulu, Hawaii.
5. Michael T. Tong, Scott M. Jones, and Philip C. Arcara, Jr., "A Probabilistic Assessment of NASA Ultra-Efficient Engine Technologies for a Large Subsonic Transport," Proceedings of Turbo Expo 2004, GT2004–53485.
6. Dongming Zhu and Robert A. Miller, "Low Conductivity and High Toughness Tetragonal Phase Structured Ceramic Thermal Barrier Coatings," US Provisional Patent Application No.: 60/712,613, August 26, 2005. US Patent Application No.: 11/510,574, August 28, 2006.
7. Dongming Zhu, Maria A. Kuczmarski, Robert A. Miller, and Michael D. Cuy, "Evaluation of Erosion Resistance of Advanced Turbine Thermal Barrier Coatings," The 31st International Cocoa Beach Conference & Exposition on Advanced Ceramics & Composites, Daytona Beach, January 22–26, 2007.
8. ANSI/ASME MFC-3M-2004, "Measurement of Fluid Flow in Pipes Using Orifice, Nozzle, and Venturi, Includes Addenda A," American Society of Mechanical Engineers/01-Jan-2004/92 pages ISBN: 0791829286.
9. Robert F. Handschuh, "High Temperature Erosion of Plasma-Sprayed Yttria-Stabilized Zirconia in a Simulated Turbine Environment," NASA TP 2406; AVSCOM TR-84-C-17, December 1984. Also AIAA–85–1219.
10. Robert W. Bruce et al., "Development of 1232 °C (2250 °F) Erosion and Impact Tests for Thermal Barrier Coatings," Tribology Transactions, vol. 44 (1998), 3990410.

REPORT DOCUMENTATION PAGE		Form Approved OMB No. 0704-0188

1. REPORT DATE *(DD-MM-YYYY)*	2. REPORT TYPE	3. DATES COVERED *(From - To)*
01-02-2010	Technical Memorandum	

4. TITLE AND SUBTITLE
Development and Life Prediction of Erosion Resistant Turbine Low Conductivity Thermal Barrier Coatings

5a. CONTRACT NUMBER

5b. GRANT NUMBER

5c. PROGRAM ELEMENT NUMBER

6. AUTHOR(S)
Zhu, Dongming; Miller, Robert, A.; Kuczmarski, Maria, A.

5d. PROJECT NUMBER

5e. TASK NUMBER

5f. WORK UNIT NUMBER
WBS 877868.02.07.03.05.01.02

7. PERFORMING ORGANIZATION NAME(S) AND ADDRESS(ES)
National Aeronautics and Space Administration
John H. Glenn Research Center at Lewis Field
Cleveland, Ohio 44135-3191

8. PERFORMING ORGANIZATION REPORT NUMBER
E-17011

9. SPONSORING/MONITORING AGENCY NAME(S) AND ADDRESS(ES)
National Aeronautics and Space Administration
Washington, DC 20546-0001

10. SPONSORING/MONITOR'S ACRONYM(S)
NASA

11. SPONSORING/MONITORING REPORT NUMBER
NASA/TM-2010-215669

12. DISTRIBUTION/AVAILABILITY STATEMENT
Unclassified-Unlimited
Subject Categories: 23, 24, and 27
Available electronically at http://gltrs.grc.nasa.gov
This publication is available from the NASA Center for AeroSpace Information, 443-757-5802

13. SUPPLEMENTARY NOTES

14. ABSTRACT
Future rotorcraft propulsion systems are required to operate under highly-loaded conditions and in harsh sand erosion environments, thereby imposing significant material design and durability issues. The incorporation of advanced thermal barrier coatings (TBC) in high pressure turbine systems enables engine designs with higher inlet temperatures, thus improving the engine efficiency, power density and reliability. The impact and erosion resistance of turbine thermal barrier coating systems are crucial to the turbine coating technology application, because a robust turbine blade TBC system is a prerequisite for fully utilizing the potential coating technology benefit in the rotorcraft propulsion. This paper describes the turbine blade TBC development in addressing the coating impact and erosion resistance. Advanced thermal barrier coating systems with improved performance have also been validated in laboratory simulated engine erosion and/or thermal gradient environments. A preliminary life prediction modeling approach to emphasize the turbine blade coating erosion is also presented.

15. SUBJECT TERMS
Thermal barrier coatings; Erosion; Life prediction; Turbine engine; Computational fluid dynamics; Burner rig testing

16. SECURITY CLASSIFICATION OF:			17. LIMITATION OF ABSTRACT	18. NUMBER OF PAGES	19a. NAME OF RESPONSIBLE PERSON
a. REPORT	b. ABSTRACT	c. THIS PAGE			STI Help Desk (email:help@sti.nasa.gov)
U	U	U	UU	14	19b. TELEPHONE NUMBER *(include area code)* 443-757-5802